

## AN EXPERIMENTAL AND THEORETICAL STUDY ON SIDEROL ISOLATED FROM *Sideritis* SPECIES

Akin AZIZOGLU<sup>1,\*</sup>, Zuleyha ÖZER<sup>2</sup> and Turgut KILIÇ<sup>3</sup>

Balikesir University, Faculty of Science and Literature, Department of Chemistry,

Division of Organic Chemistry, 10145 Balikesir, Turkey;

e-mail: <sup>1</sup> azizoglu@balikesir.edu.tr, <sup>2</sup> zuleyha.ozer@hotmail.com, <sup>3</sup> tkilic@balikesir.edu.tr

Received September 23, 2010

Accepted December 6, 2010

Published online January 25, 2011

The Fourier transform infrared (FTIR) spectrum of siderol, extracted from the aerial parts of *Sideritis Gülandamii*, has been measured in the range 4000–400 cm<sup>-1</sup>. Vibrational assignments and analyses of the fundamental modes of siderol were performed using the observed FTIR data recorded in the solid phase. The vibrational frequencies determined experimentally are compared with those obtained theoretically from density functional theory (DFT) and Hartree–Fock (HF) calculations. Optimized geometrical parameters of the title compound are in agreement with similar reported structures. The <sup>1</sup>H and <sup>13</sup>C NMR spectra of siderol have also been calculated by means of DFT and HF methods. The comparison between the experimental and the theoretical results indicates that density functional methods, B3LYP and MPW1PW91 with 6-31G(d) basis set, are able to provide satisfactory results for predicting NMR properties. On the basis of vibrational analyses, the thermodynamic properties of the title molecule have also been computed.

**Keywords:** Terpenoids; Natural Products; Density functional calculations; *Ab initio* calculations.

The chemistry and structure of natural products have been an interesting field of study for a long time. Especially, terpenes and terpenoids are one of the main groups of secondary metabolites in nature, showing a great diversity in structure and activity<sup>1,2</sup>. They can also be used as intermediates and ingredients for flavours, fragrances and pharmaceuticals. Hence, researches on these compounds have lately undergone exponential growth due to advances in isolation techniques and synthetic method design, as well as the finding of a wide range of biological properties exhibited by them<sup>3,4</sup>. Siderol (**1**), one of the kaurene terpenoids (Fig. 1), is isolated from the genus *Sideritis* (Lamiaceae) distributed mainly in the in temperate and tropical regions of the Northern Hemisphere, particularly in the Mediterranean and

the Middle East<sup>5,6</sup>. It has the antibacterial and antiviral activity against different bacteria<sup>7</sup>.

Computational methods are increasingly applied to representative biological active compounds aiming to elucidate their molecular structures and electronic properties, which contribute to the recognition of structure-activity relationships and to the understanding of the properties and system behavior<sup>8–10</sup>. More recently, several investigations have been carried out on the biological active molecules isolated from plants<sup>11,12</sup>. Literature survey reveals that to the best of our knowledge no *ab initio* density functional theory (DFT) and Hartree–Fock (HF) calculations of siderol have been reported so far. It may be due to difficulty in interpreting the results of calculations because of their complexity and low symmetry. Herein, we wish to report the optimal geometry and the detailed vibrational spectrum of siderol with the help of theoretical and experimental methods. In addition, the gauge-including atomic orbital (GIAO) <sup>1</sup>H and <sup>13</sup>C chemical shifts calculations of the title compound have been analyzed using HF and DFT methods. The spectroscopic constants derived from the *ab initio* HF and DFT calculations have been compared with the corresponding values obtained from the experimental studies.

## RESULTS AND DISCUSSION

The general route for the isolation of siderol is described in the part of experimental methods. The geometry optimization is the most important step for the calculation of the NMR and IR spectra because the molecular parameters are controlled by the molecular geometry. The general molecular structure and numbering of the atoms of siderol is shown in Fig. 1. The molecular geometry of the title compound has been optimized at the RHF-SCF, DFT/B3LYP and DFT/MPW1PW91 level of theories in the ground state (*in vacuo*).

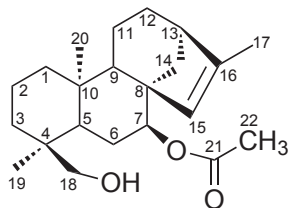


FIG. 1  
Structure and atom numbering scheme of siderol (1)

The geometry of siderol obtained from the optimization with B3LYP/6-31G(d) method is depicted in Fig. 2. The results of optimized parameters (bond lengths, bond angles and dihedral angles) of siderol are also listed in Table I. Since the crystal structure of siderol is not available and our crystallization efforts in various solvent systems failed, the optimized structure can be only being compared with other similar systems for which X-ray structures have been reported recently<sup>13,14</sup>. For example, the optimized bond lengths of C4–C5, C6–C7 and C13–C14 in siderol are 1.565, 1.523 and 1.5304 Å for RHF/6-31G(d) method, 1.560, 1.522 and 1.530 Å for RMPW1PW91/6-31G(d) method, and 1.571, 1.529 and 1.538 Å for RB3LYP/6-31G(d) method, which are in good agreement with a similar molecular structure 1.563, 1.523 and 1.526 Å<sup>13</sup>. It is so remarkable that the optimized C<sub>18</sub>–O<sub>18'</sub> bond lengths by three methods are 1.407 Å for RHF/6-31G(d), 1.418 Å for RMPW1PW91/6-31G(d) and 1.430 Å for RB3LYP/6-31G(d), which are slightly shorter than that in compound with a similar molecular structure 1.432 Å. However, they are 1.453 Å for RHF/3-21G(d), 1.468 for RMPW1PW91/3-21G(d) and 1.480 for RB3LYP/3-21G(d), which are significantly longer than this value<sup>13</sup>. Moreover, the optimized O<sub>21</sub>=C<sub>21'</sub> carbonyl group bond lengths obtained from RHF/6-31G(d), RMPW1PW91/6-31G(d) and RB3LYP/6-31G(d) methods are 1.190, 1.209 and 1.219 Å, respectively, which are in good agreement with a similar structure 1.181 Å, whereas those achieved by RHF/3-21G(d), RMPW1PW91/3-21G(d) and RB3LYP/3-21G(d) methods are 1.206, 1.224 and 1.227 Å, respectively, which are again longer than the experimental values of similar structure<sup>14</sup>.

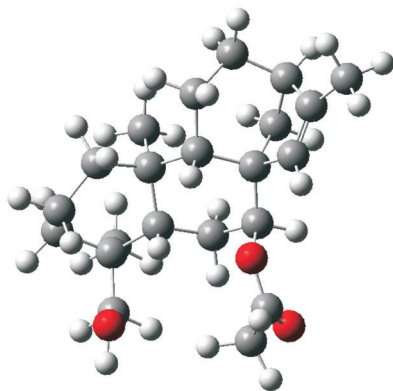


FIG. 2  
Optimized structure of siderol achieved by B3LYP/6-31G(d) method

TABLE I  
Optimized geometrical structural parameters (bond lengths (in Å), bond angles (in °) and dihedral angles (in °)) of siderol

Parameter	HF		DFT			
	RHF/ 6-31G(d)	RHF/ 3-21G(d)	RMPW1PW91 6-31G(d)	RMPW1PW91 3-21G(d)	RB3LYP/ 6-31G(d)	RB3LYP/ 3-21G(d)
Bond length						
C4–C5	1.565	1.561	1.560	1.556	1.571	1.569
C4–C18	1.540	1.541	1.537	1.539	1.546	1.548
O18'–C18	1.407	1.453	1.418	1.468	1.430	1.480
H–O18'	0.947	0.966	0.964	0.988	0.969	0.993
C3–C4	1.552	1.553	1.549	1.549	1.558	1.559
O21'=C21	1.190	1.206	1.209	1.224	1.219	1.227
C21–O21'	1.332	1.354	1.342	1.379	1.351	1.389
O7'–C21'	1.438	1.470	1.449	1.488	1.462	1.501
C21–C22	1.505	1.500	1.505	1.501	1.512	1.509
C6–C7	1.523	1.528	1.522	1.527	1.529	1.535
C8–C16	1.529	1.531	1.523	1.529	1.531	1.537
C15–C16	1.321	1.320	1.337	1.337	1.339	1.338
C15–C17	1.499	1.501	1.491	1.496	1.497	1.503
C13–C15	1.522	1.531	1.520	1.531	1.528	1.539
C13–C14	1.530	1.541	1.530	1.541	1.538	1.549
C8–C14	1.545	1.549	1.543	1.547	1.553	1.557
Bond angle						
C16–C15–C17	128.1	128.4	128.3	128.6	128.2	128.5
H17'–C17–C15	111.5	111.3	111.7	111.3	111.7	111.3
C21–O7'–C7	119.5	119.8	117.3	115.9	117.7	116.1
C22–C21–O7'	111.1	110.5	110.5	109.4	110.4	109.2
O21'–C21–C22	124.6	126.7	125.1	127.5	125.1	127.6
O7'–C7–C8	107.1	105.5	106.9	105.3	106.9	105.2
H18'–O18'–C18	109.2	110.7	107.6	108.3	107.5	108.0
H19'–C18–O18'	109.8	109.4	110.3	110.0	110.1	110.0
O18'–C18–C4	111.4	110.3	110.9	110.0	111.0	110.0
C5–C6–C7	111.3	109.5	111.1	109.3	111.1	109.4
O21'–C21–O7'	124.3	122.7	124.3	123.0	124.4	123.0

TABLE I  
(Continued)

Parameter	HF		DFT			
	RHF/ 6-31G(d)	RHF/ 3-21G(d)	RMPW1PW91 6-31G(d)	RMPW1PW91 3-21G(d)	RB3LYP/ 6-31G(d)	RB3LYP/ 3-21G(d)
Dihedral angle						
C13–C15–C16–C8	0.27	–0.47	0.01	0.95	0.05	0.79
C15–C16–C8–C7	–90.0	–90.4	–89.8	–89.9	–89.7	–89.8
C15–C13–C12–C11	–50.9	–49.0	–50.0	–47.8	–50.2	–48.1
C17–C15–C16–C8	176.1	175.6	175.1	173.9	175.6	174.5
H15'–C16–C15–C17	1.03	0.56	0.95	0.29	1.01	0.41
C15–C13–C14–C8	41.4	40.1	41.3	39.9	41.4	40.1
H7'–C7–O7'–C21	–41.4	–53.1	–43.3	–53.7	–43.7	–52.5
O21'–C21–O7'–C7	2.91	12.5	4.78	13.8	6.55	13.8
C21–O7'–C7–C6	78.6	67.9	76.8	67.4	76.2	68.3
H22'–C22–C21–O(C=O)	6.3	18.7	12.8	22.4	14.5	22.0
O18'–C18–C4–C19	176.8	180.0	177.9	179.5	178.8	178.7
O18'–C18–C4–C5	60.2	57.1	58.4	57.0	58.4	56.0

### Vibrational Analysis

The experimental and theoretical IR spectra are shown in Fig. 3 for comparative purposes, where the calculated intensity and activity are plotted against the harmonic vibrational frequencies. The experimental and calculated wavenumbers and IR intensities are also given in Table II. In order to facilitate assignment of the observed peaks, we have analyzed vibrational frequencies and compared our calculation of the compound with their experimental results. The vibrational frequency and approximate description of each normal mode obtained using HF and DFT methods with both 6-31G(d) and 3-21G(d) basis sets. The assignment of the experimental frequencies are based on the observed band frequencies in the infrared spectrum of this species confirmed by establishing "one to one" correlation between experiment and theory.

The calculated vibrational spectra of the title molecule belonging to  $C_1$  point group have no imaginary frequencies which helped to confirm that the structure of the compound deduced following geometry optimization corresponds to energy minimum. In total, there are 171 vibrations from 49

to  $3880\text{ cm}^{-1}$  at RHF/3-21G(d) level, 37 to  $4115\text{ cm}^{-1}$  at RHF/6-31G(d) level, 54 to  $3503\text{ cm}^{-1}$  at B3LYP/3-21G(d) level, 41 to  $3757\text{ cm}^{-1}$  at B3LYP/6-31G(d) level, 54 to  $3589\text{ cm}^{-1}$  at MPW1PW91/3-21G(d) level and 39 to  $3831\text{ cm}^{-1}$  at MPW1PW91/6-31G(d) level. The main focus of the present investigation is the proper assignment of the experimental frequencies to the various vibrational modes of siderol in corroboration with the calculated harmonic frequencies at HF, B3LYP and MPW1PW91 levels using both 3-21G(d) and 6-31G(d) basis sets. To make comparison with experiment, we obtained the correlation graphics, from which the correlation values of computational and experimental frequencies are found to be 0.995 for RHF/3-21G(d), 0.9838 for RHF/6-31G(d), 0.9971 for RB3LYP/3-21G(d),

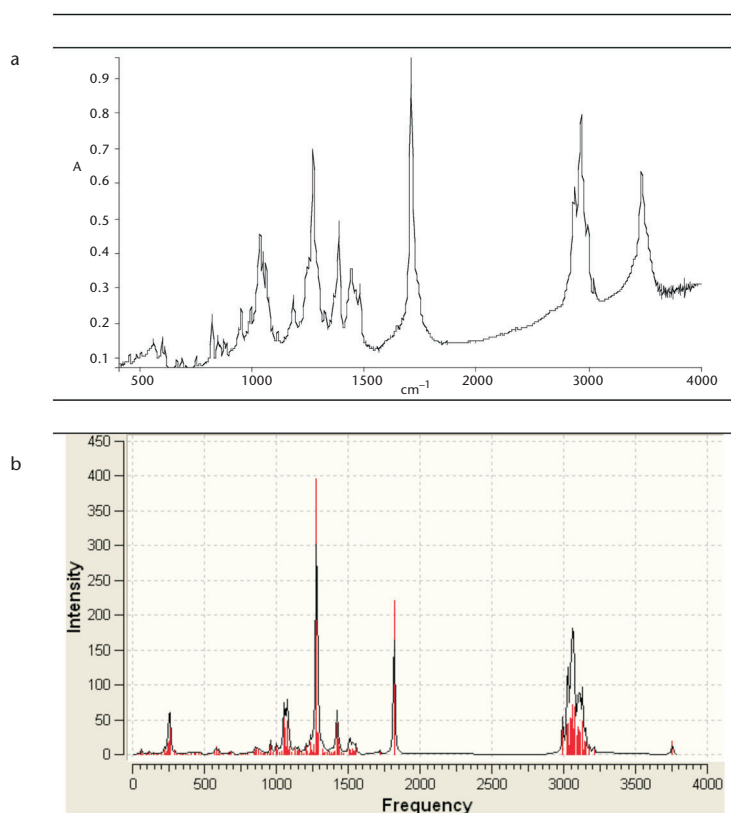


FIG. 3  
Experimental (a) and calculated (b) IR spectrum (RB3LYP/6-31G(d)) of siderol

0.9938 for RB3LYP/6-31G(d), 0.995 for RMPW1PW91/3-21G(d) and 0.9958 for RMPW1PW91/6-31G(d) level, respectively. Hence, experimental fundamentals have slightly a better correlation for RB3LYP/3-21G(d) than the others (Fig. 4).

Generally, the calculated frequencies are slightly higher than the observed values for the majority of the normal modes. Two factors may be responsible for the discrepancies between the experimental and computed spectra of the title molecule. The first is caused by the environment and the second reason for these discrepancies is the fact that the experimental value is an anharmonic frequency while the calculated value is a harmonic one<sup>15</sup>.

In the experimental spectrum, C–C vibrations in siderol arise from mainly C=C bond of bicycloalkene and methyl and cyclohexyl carbons. The weak intense IR band at  $1645\text{ cm}^{-1}$  is assigned to the  $C_{15}=C_{16}$  bond stretching. As seen from Table II, the medium intense band at around  $948\text{ cm}^{-1}$  can also be assigned to the C–C bond stretching and CCC in plane deformation. The C–H stretching vibration bands are at  $3050\text{--}2800\text{ cm}^{-1}$  (see Fig. 3). This interval can be divided into two parts: the first one between  $3050$  and  $3010\text{ cm}^{-1}$  corresponds to the stretch vibration of the double bond C–H and the other one at  $3010\text{--}2800\text{ cm}^{-1}$  to the saturated aliphatic CH groups. Moreover, C=C–CH<sub>3</sub> scissoring vibrations are identified in the range of  $1655\text{--}1510\text{ cm}^{-1}$  by DFT and HF methods and it is in agreement with the recorded FTIR spectral value of  $1558\text{ cm}^{-1}$  except HF/3-21G(d) level ( $1655\text{ cm}^{-1}$ ). The O=C–CH<sub>3</sub> wagging vibration computed

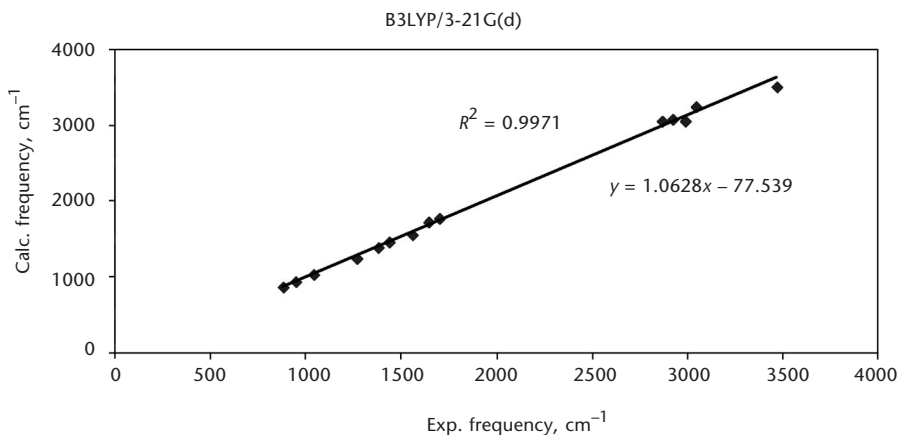


FIG. 4  
Correlation graphics of calculated versus experimental frequencies of siderol

TABLE II  
Selected experimental and theoretical vibrational wavenumbers (in  $\text{cm}^{-1}$ ) of siderol

Experimental	HF/6-31G(d)	HF/3-21G(d)	B3LYP/6-31G(d)	B3LYP/3-21G(d)	MPW1PW91/ 6-31G(d)	MPW1PW91/ 3-21G(d)	Approximate description
881	283, 642	209	259	197	262	207	O-H rocking
948	966	935	857	868	858	894	C=C-H out of plane bending
1032, 1044,	983	964	962	923	981	978	C-C symmetrical stretch and CCC in plane deformation
1057	1336, 1349,	919, 935	1263, 1266,	1025, 1032,	1080, 1084,	1263, 1270,	C-H rocking
1268	1370	945	1321	1046	1090	1291	C-O symmetrical stretch
1383	1427	1371	1280	1227	1310	1255	C-H wagging
1439	1371	1351	1393	1381	1329	1395	O=C-CH <sub>3</sub> wagging
1558	1427	1573	1421	1458	1434	1458	C=C-CH <sub>3</sub> scissoring
	1566	1655	1517	1549	1510	1548	C=C-CH <sub>3</sub> wagging
	1559	1577	1441	1555	1443	1462	H-O-CH <sub>2</sub> wagging
		1642	1473			1467	O=C-CH <sub>3</sub> scissoring
1645		1658.1	1507	1560	1506	1546	H-O-CH <sub>2</sub> scissoring
1708	1879	1858	1550	1573			C=C symmetrical stretch
	2002	1927	1721	1706	1745	1728	C=O symmetrical stretch
2873	3184	3189	1820	1754	1856	1785	H-O-CH <sub>2</sub> symmetrical stretch
2992	3221	3239	2994	3015	3015	3033	H-O-CH <sub>2</sub> asymmetrical stretch
2930	3209	3203	3025	3058	3054	3081	C-H symmetrical stretch
	3231	3268	3061	3039	3082	3059	C-H asymmetrical stretch
	3228		3064	3081	3131	3108	O=C-CH <sub>3</sub> symmetrical stretch
	3290		3066	3044	3096	3064	C-O-C-H symmetrical stretch
	3234.4	3258	3093		3115		C=C-CH <sub>3</sub> asymmetrical stretch
3046	3294	3407	3117	3067	3157	3148	O=C-CH <sub>3</sub> asymmetrical stretch
3473	3389	3880	3179	3136	3174	3166	C=C-H symmetrical stretch
	4115		3212	3236	3241	3262	O-H symmetrical stretch
			3757	3503	3831	3588	O-H asymmetrical stretch



by MPW1PW91/6-31G(d) method is around  $1434\text{ cm}^{-1}$  and it shows better agreement with the experimentally observed value of  $1439\text{ cm}^{-1}$  than the others.

The free OH group absorbs strongly in the region of  $3700\text{--}3580\text{ cm}^{-1}$ , whereas the existence of intermolecular hydrogen bond formation can lower the O–H stretching frequency to the  $3550\text{--}3200\text{ cm}^{-1}$  region with increase in intensity and breath<sup>16</sup>. The IR spectrum in the high wavenumber region shows a sharp intense band at  $3473\text{ cm}^{-1}$ , attributed to no hydrogen bonded OH stretching vibrations. It is possible that the OH group may participate in intermolecular hydrogen bonding with a neighboring molecule. Due to that, the calculated values of OH group vibrations,  $4115\text{ cm}^{-1}$  for HF/6-31G(d),  $3880\text{ cm}^{-1}$  for HF/3-21G(d),  $3757\text{ cm}^{-1}$  for B3LYP/6-31G(d) and  $3831\text{ cm}^{-1}$  for MPW1PW91/6-31G(d), show no good agreement with the experimental results except of  $3503\text{ cm}^{-1}$  for B3LYP/3-21G(d) and  $3588\text{ cm}^{-1}$  for MPW1PW91/3-21G(d).

Normal esters are characterized by the strong IR absorptions due to the C=O stretching vibration in the range of  $1750\text{--}1735\text{ cm}^{-1}$  and the other due to C–O stretching vibration near  $1200\text{ cm}^{-1}$ . Similarly in our study also a strong band observed by IR at  $1708\text{ cm}^{-1}$  is assigned to C=O stretching vibration. However, the theoretically computed one by HF/6-31G(d) and HF/3-31G(d) shows great deviation of about  $294$  and  $219\text{ cm}^{-1}$ , respectively. DFT methods have a better correlation with the recorded spectrum. This deviation may be due to the presence of CH<sub>2</sub>OH group in the adjacent position. The other characteristic carboxylic group vibration is the C–O stretching at  $1268\text{ cm}^{-1}$ . The computed values are at  $1427$ ,  $1371$ ,  $1280$ ,  $1227$ ,  $1310$  and  $1255\text{ cm}^{-1}$  by HF/6-31G(d), HF/3-21G(d), B3LYP/6-31G(d), B3LYP/3-21G(d), MPW1PW91/6-31G(d) and MPW1PW91/3-21G(d), respectively. DFT methods again show a better agreement with experimental observation than HF methods.

### *NMR Spectra*

GIAO <sup>1</sup>H and <sup>13</sup>C chemical shift values (with respect to TMS) have been calculated using DFT and HF methods with both 3-21G(d) and 6-31G(d) basis sets and generally compared to the experimental <sup>1</sup>H and <sup>13</sup>C chemical shift values reported in ppm relative to TMS. The experimental and computed NMR results are shown in Tables III and IV. Experimental <sup>1</sup>H and <sup>13</sup>C NMR spectra were obtained at a base frequency of  $500\text{ MHz}$  for <sup>1</sup>H and  $125\text{ MHz}$  for <sup>13</sup>C nuclei. Relative chemical shifts were then estimated using the corresponding TMS shielding calculated in advance at the same theoretical

level as the reference. Calculated  $^1\text{H}$  isotropic chemical shift values for TMS at RHF/3-21G(d), RHF/6-31G(d), B3LYP/3-21G(d), B3LYP/6-31G(d), MPW1PW91/3-21G(d) and MPW1PW91/6-31G(d) levels were 33.6, 32.9, 32.8, 32.2, 32.7 and 32.2 ppm, respectively. Moreover, calculated  $^{13}\text{C}$  chemical shift values for TMS at RHF/3-21G(d), RHF/6-31G(d), B3LYP/3-21G(d), B3LYP/6-31G(d), MPW1PW91/3-21G(d) and MPW1PW91/6-31G(d) levels were 213.2, 201.7, 201.8, 189.7, 205.8 and 194.3 ppm, respectively. The ex-

TABLE III  
Experimental and calculated  $^{13}\text{C}$  NMR chemical shifts (in ppm) of siderol

Carbon No.	Exp.	DFT				HF	
		MPW1PW91/6-31G(d)	MPW1PW91/3-21G(d)	B3LYP/6-31G(d)	B3LYP/3-21G(d)	HF/6-31G(d)	HF/3-21G(d)
C <sub>1</sub>	42.0	40.0	36.6	40.9	37.7	34.8	32.6
C <sub>2</sub>	18.4	21.4	19.6	22.2	20.9	18.0	15.7
C <sub>3</sub>	35.4	35.0	32.9	36.3	34.5	30.4	28.8
C <sub>4</sub>	36.9	35.5	34.0	38.4	37.5	30.1	29.0
C <sub>5</sub>	44.5	32.0	29.5	33.9	31.9	26.8	25.1
C <sub>6</sub>	23.6	24.1	21.5	24.9	22.7	21.9	19.0
C <sub>7</sub>	78.4	75.7	73.2	78.0	72.8	68.5	67.0
C <sub>8</sub>	51.8	51.4	48.7	53.9	51.5	44.6	42.9
C <sub>9</sub>	44.9	44.0	40.2	46.7	43.2	38.5	35.4
C <sub>10</sub>	39.2	38.3	36.2	41.6	39.9	31.8	30.2
C <sub>11</sub>	17.9	20.8	20.0	22.0	21.5	17.9	16.7
C <sub>12</sub>	24.7	26.1	23.4	27.4	24.9	22.4	19.8
C <sub>13</sub>	39.8	44.0	41.4	45.5	43.4	38.1	36.2
C <sub>14</sub>	39.8	42.8	37.8	44.0	39.2	37.8	34.3
C <sub>15</sub>	145.8	138.8	127.0	138.4	201.7	140.0	131.1
C <sub>16</sub>	130.0	129.0	120.1	128.2	201.7	129.5	124.5
C <sub>17</sub>	15.4	17.0	16.4	16.9	16.5	16.4	15.6
C <sub>18</sub>	71.4	72.1	69.2	73.4	71.1	64.8	62.8
C <sub>19</sub>	17.6	22.9	20.5	22.9	20.8	20.9	19.1
C <sub>20</sub>	17.9	26.1	23.6	25.7	23.4	23.0	21.1
C <sub>21</sub>	171.1	161.5	159.7	160.8	201.7	162.9	166.8
C <sub>22</sub>	21.0	21.5	20.7	21.0	20.5	21.9	20.9

TABLE IV  
 Experimental and calculated  $^1\text{H}$  NMR chemical shifts (in ppm) of siderol

Proton No.	Exp.	DFT				HF	
		MPW1PW91/ 6-31G(d)	MPW1PW91/ 3-21G(d)	B3LYP/ 6-31G(d)	B3LYP/ 3-21G(d)	HF/ 6-31G(d)	HF/ 3-21G(d)
H(2'a)	–	2.33	2.70	2.32	2.68	1.99	2.20
H(2'b)	–	1.38	1.05	1.40	1.10	1.20	0.88
H(3'a)	–	1.59	1.43	1.60	1.48	1.24	1.03
H(3'b)	–	1.70	1.23	1.71	1.27	1.44	1.01
H(1'a)	–	1.46	1.35	1.47	1.39	1.15	1.02
H(1'b)	–	1.55	1.38	1.56	1.42	1.21	1.05
H(5')	–	2.85	2.95	2.90	3.03	2.15	2.18
H(9')	–	1.89	1.75	1.95	1.81	1.43	1.35
H(7')	4.6	4.57	4.44	4.62	4.51	4.20	4.13
H(6'a)	–	2.12	2.06	2.09	2.04	1.78	1.66
H(6'b)	–	1.46	1.22	1.46	1.26	1.04	0.73
H(11'a)	–	1.75	1.58	1.81	1.66	1.41	1.24
H(11'b)	–	1.56	1.29	1.56	1.32	1.20	0.91
H(12'a)	–	1.52	1.25	1.56	1.32	1.33	1.05
H(12'b)	–	1.56	1.30	1.57	1.33	1.29	0.98
H(13')	2.37	2.31	1.98	2.31	2.01	2.00	1.74
H(14'a)	–	1.61	1.55	1.59	1.55	1.30	1.26
H(14'b)	–	1.92	1.72	1.91	1.74	1.47	1.26
H(15')	5.25	5.70	5.67	5.63	5.64	5.77	5.94
H(17'a)	1.01	1.65	1.60	1.69	1.64	1.56	1.51
H(17'b)	1.01	1.82	1.70	1.78	1.69	1.84	1.74
H(17'c)	1.01	1.64	1.59	1.64	1.60	1.57	1.54
H(18'a)	2.98	3.12	2.95	3.17	3.05	2.85	2.68
H(18'b)	3.31	3.66	3.67	3.73	3.79	3.27	3.25
H(19'a)	0.67	0.56	0.53	0.57	0.60	0.46	0.38
H(19'b)	0.67	0.40	0.25	0.40	0.29	0.37	0.19
H(19'c)	0.67	1.09	1.04	1.04	1.03	0.96	0.90
H(O)	–	0.04	0.49	0.12	0.64	–0.10	0.001
H(22'a)	2.05	1.51	1.40	1.45	1.35	1.61	1.59
H(22'b)	2.05	1.97	2.10	1.95	2.08	1.96	2.11
H(22'c)	2.05	2.18	3.41	2.22	3.44	2.14	3.05
H(20'a)	1.11	1.22	1.16	1.19	1.14	0.98	0.90
H(20'b)	1.11	1.13	1.05	1.10	1.06	0.88	0.76
H(20'c)	1.11	1.56	1.55	1.54	1.57	1.14	1.08

perimental values for  $^1\text{H}$  and  $^{13}\text{C}$  isotropic chemical shifts for TMS were 30.8 and 188.1 ppm, respectively<sup>17</sup>.

As can be seen from Tables III and IV, the calculated chemical shifts are in compliance with the experimental findings. Comparing calculated and experimental data, the correlation values of carbon and proton shifts are found to be 0.9862 and 0.8846 for RHF/3-21G(d), 0.9872 and 0.925 for RHF/6-31G(d), 0.9542 and 0.884 for B3LYP/3-21G(d), 0.993 and 0.9364 for

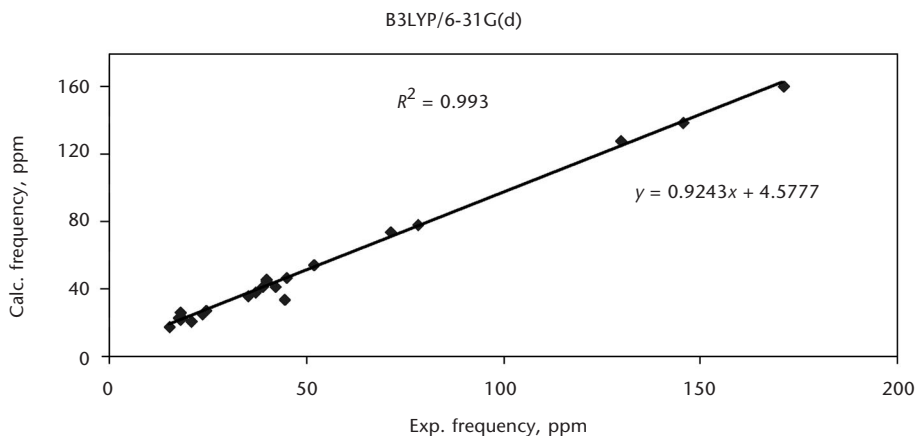


FIG. 5  
Correlation graphics of calculated versus experimental  $^{13}\text{C}$  NMR frequencies of siderol

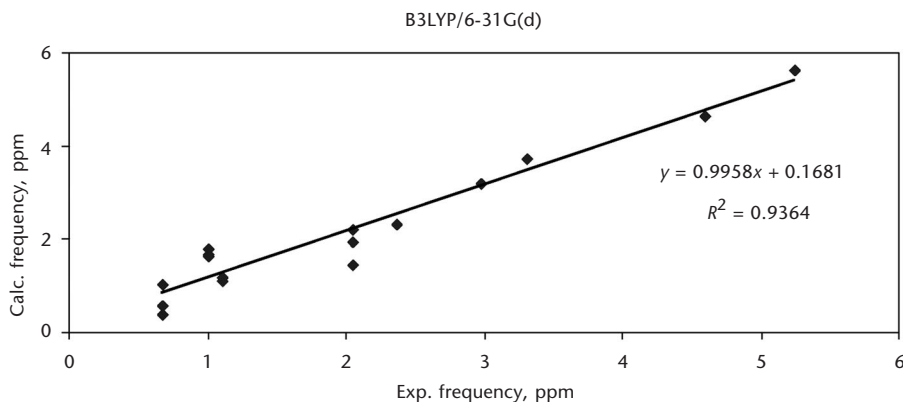


FIG. 6  
Correlation graphics of calculated versus experimental  $^1\text{H}$  NMR frequencies of siderol

B3LYP/6-31G(d), 0.9909 and 0.8842 for MPW1PW91/3-21G(d), 0.992 and 0.9359 for MPW1PW91/6-31G(d) level, respectively (best ones in Figs 5 and 6). Hence, the results of DFT methods with 6-31G(d) basis set have shown better fit to experimental ones than HF methods in evaluating  $^1\text{H}$  and  $^{13}\text{C}$  chemical shifts.

The proton of double bond (H-15') resonates at 5.25 ppm from  $^1\text{H}$  NMR spectrum of the title compound (Fig. 7). This signal has been calculated as

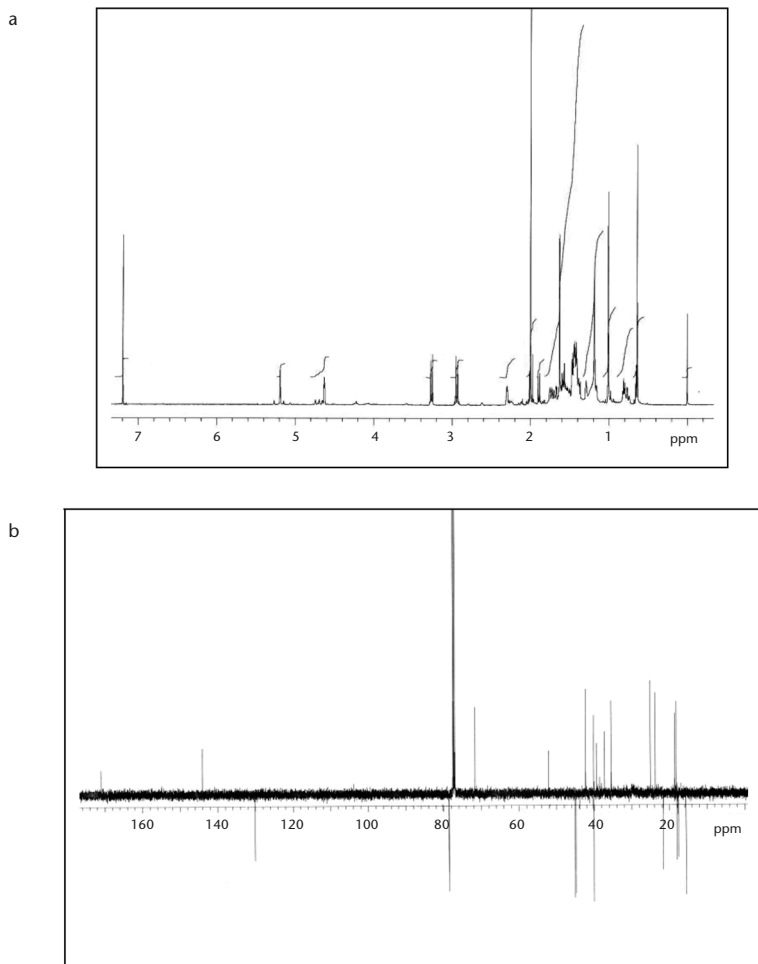


FIG. 7  
 $^1\text{H}$  (500 MHz; a) and  $^{13}\text{C}$  NMR (125 MHz, APT technique; b) of siderol in  $\text{CDCl}_3$

5.63 ppm (best) for B3LYP/6-31G(d) and 5.94 ppm (worst) for HF/3-21G(d). The signal at 4.60 ppm is also assigned to H atom attached to C-7. It has been computed as 4.62 ppm (best) for B3LYP/6-31G(d) and 4.13 ppm (worst) for HF/3-21G(d). Moreover,  $^{13}\text{C}$  NMR spectrum of siderol shows the signal at 171.1 ppm experimentally, that has been calculated at 159.7–201.7 ppm due to the C atom of carbonyl group.

### *Frontier Molecular Orbitals*

Frontier molecular orbital (MO) theory in chemistry is an application of MO theory describing highest occupied MO (HOMO)/lowest unoccupied MO (LUMO) interactions that play an important role in the electric, optical and other properties, as well as in UV-Vis spectra and chemical reactions<sup>18</sup>. Figure 8 indicates the distribution and energy levels of the HOMO-1, HOMO, LUMO, LUMO+1 orbitals calculated at B3LYP/6-31G(d) level for siderol. As seen from Fig. 8, HOMO and LUMO+1 are mainly on the double bond, whereas LUMO are substantially localized on the carbonyl group. Electrons in the HOMO-1 are also delocalized through the molecule. The value of energy separation between HOMO and LUMO is 0.241 eV. This small HOMO-LUMO gap means low excitation energies for many of excited states and low chemical hardness for siderol.

### *Other Molecular Properties*

The calculation of effective atomic charges plays an important role in the application of quantum mechanical calculations to molecular systems. Natural population analysis (NPA) atomic charges for the non-H atoms of the title compound calculated at MPW1PW91/3-21G(d), MPW1PW91/6-31G(d), B3LYP/3-21G(d), B3LYP/6-31G(d), RHF/3-21G(d) and RHF/6-31G(d) levels are presented in Table V. Generally, the computed results show that the carbon atom of carbonyl group has a bigger positive charge and carbon atom of methyl group attached to carbonyl has a bigger negative charge. Moreover, the large negative charge of oxygen atom of hydroxy group may be regarded as a nucleophilic suction pump, acting as a possible magnet for electrophilic attack of  $\text{H}^+$  or part of a biological receptor.

The thermodynamic parameters of the title compound have been also calculated at MPW1PW91/3-21G(d), MPW1PW91/6-31G(d), B3LYP/3-21G(d), B3LYP/6-31G(d), RHF/3-21G(d) and RHF/6-31G(d) levels and are presented in Table VI. These results will be helpful for further studies of siderol.

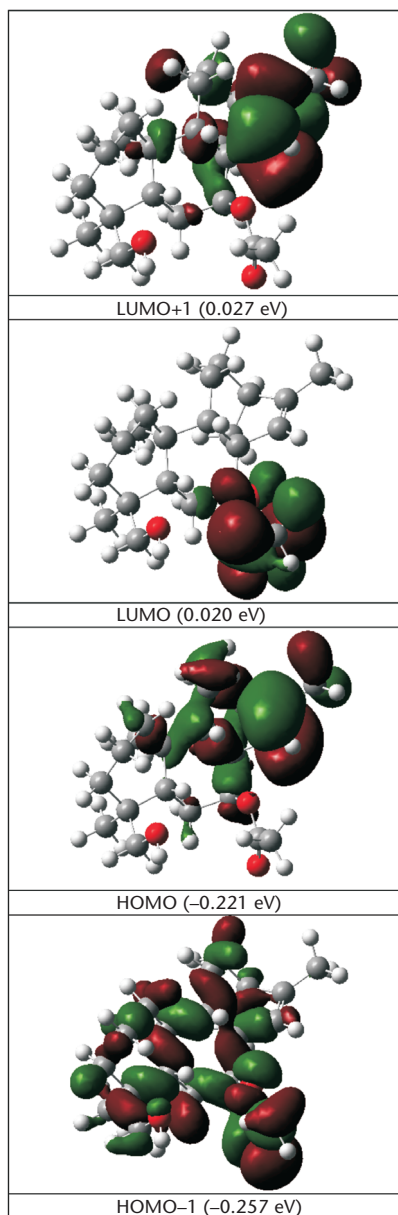


FIG. 8  
LUMO+1, LUMO, HOMO and HOMO-1 orbitals of siderol

TABLE V  
NPA atomic charges (in  $\_$ ) of siderol at the DFT and HF methods with both 6-31G(d) and 3-21G(d) basis sets

Atom No.	DFT				HF	
	MPW1PW91/ 6-31G(d)	MPW1PW91/ 3-21G(d)	B3LYP/ 6-31G(d)	B3LYP/ 3-21G(d)	HF/ 6-31G(d)	HF/ 3-21G(d)
C1	-0.466	-0.468	-0.448	-0.448	-0.416	-0.433
C2	-0.480	-0.495	-0.460	-0.473	-0.427	-0.460
C3	-0.470	-0.468	-0.451	-0.448	-0.420	-0.434
C4	-0.076	-0.088	-0.068	-0.079	-0.064	-0.085
C5	-0.283	-0.279	-0.270	-0.266	-0.254	-0.260
C6	-0.495	-0.503	-0.476	-0.482	-0.445	-0.474
C7	0.095	0.068	0.104	0.074	0.165	0.140
C8	-0.106	-0.121	-0.099	-0.112	-0.092	-0.115
C9	-0.255	-0.250	-0.243	-0.237	-0.227	-0.229
C10	-0.051	-0.057	-0.045	-0.050	-0.040	-0.054
C11	-0.486	-0.491	-0.466	-0.470	-0.434	-0.457
C12	-0.468	-0.473	-0.449	-0.453	-0.418	-0.441
C13	-0.279	-0.288	-0.266	-0.275	-0.245	-0.267
C14	-0.452	-0.452	-0.435	-0.433	-0.406	-0.421
C15	-0.226	-0.217	-0.219	-0.209	-0.220	-0.210
C16	-0.014	-0.022	-0.012	-0.018	-0.008	-0.021
C17	-0.716	-0.727	-0.691	-0.698	-0.644	-0.674
C18	-0.099	-0.142	-0.085	-0.129	-0.014	-0.064
C19	-0.700	-0.700	-0.675	-0.673	-0.632	-0.653
C20	-0.696	-0.687	-0.671	-0.662	-0.627	-0.642
C21	0.838	0.742	0.832	0.728	0.996	0.913
C22	-0.801	-0.828	-0.773	-0.797	-0.734	-0.784
O7'	-0.573	-0.522	-0.574	-0.515	-0.670	-0.642
O18'	-0.767	-0.691	-0.765	-0.678	-0.808	-0.756
O21'	-0.611	-0.537	-0.607	-0.527	-0.710	-0.640



TABLE VI  
Calculated thermodynamic parameters of siderol employing the DFT and HF methods with both 6-31G(d) and 3-21G(d) basis sets

Parameter	DFT			HF		
	MPW1PW91/ 6-31G(d)	MPW1PW91/ 3-21G(d)	B3LYP/ 6-31G(d)	B3LYP/ 3-21G(d)	HF/ 6-31G(d)	HF/ 3-21G(d)
Thermal energy, kcal mol <sup>-1</sup>	351.45	352.39	348.70	349.79	371.84	371.35
Vibrational energy, kcal mol <sup>-1</sup>	336.37	337.63	333.52	334.87	357.64	357.29
Heat capacity, kcal mol <sup>-1</sup> K <sup>-1</sup>	97.78	97.17	98.71	98.31	91.27	91.51
Entropy, kcal mol <sup>-1</sup> K <sup>-1</sup>	159.43	155.03	159.94	155.98	154.38	151.35
Dipole moment, D	1.470	2.314	1.530	2.339	1.409	2.082
Rotational constants, GHz	0.32453 0.19798 0.14931	0.34369 0.19662 0.15350	0.32160 0.19551 0.14756	0.33802 0.19438 0.15131	0.32121 0.19701 0.14796	0.33999 0.19599 0.15232

## CONCLUSIONS

Siderol (1) characterized using spectral methods has been isolated from endemic plant, *Sideritis Gülendammii*. Geometrical structural parameters (bond lengths, bond angles, dihedral angles), vibrational frequencies, IR intensities,  $^1\text{H}$  and  $^{13}\text{C}$  NMR chemical shifts and thermodynamic parameters of siderol in the ground state have been calculated using DFT and HF methods with both 6-31G(d) and 3-21G(d) basis sets. Experimental and theoretical vibrational analyses of siderol have also been performed for the first time. Calculated vibrational frequencies have been compared with that obtained from the experimental IR spectrum. Experimental fundamentals are found to have slightly a better correlation for DFT than for HF method. Moreover,  $^1\text{H}$  and  $^{13}\text{C}$  NMR chemical shifts have been compared with experimental values. DFT results with 6-31G(d) basis set have shown a better fit to experimental ones than HF methods in evaluating  $^1\text{H}$  and  $^{13}\text{C}$  chemical shifts.

## EXPERIMENTAL

### Materials and Instruments

All solvents were purchased from Merck and Aldrich. Silica gel 60 was also used for column chromatography and Kieselgel 60F254 precoated plates (Merck Co.) for preparative TLC. The FTIR spectrum of the title compound was obtained using IR grade KBr disks on a Perkin-Elmer 1600 Series FTIR spectrophotometer in the range of  $4000\text{--}400\text{ cm}^{-1}$  at room temperature.  $^1\text{H}$  and  $^{13}\text{C}$  spectra were obtained in  $\text{CDCl}_3$  using Varian 500 MHz NMR.

### Plant Material

Siderol having the *ent*-kaurene skeleton can be isolated from different species of *Sideritis* such as *S. Trojana*, *S. Dichotoma*, *S. Sipylea Boiss*<sup>19</sup>, *S. Argyrea*<sup>20</sup>, *S. Lycia*, *S. Gülendammiae H. Duman*  $\delta$  *F. A. Karaveliogullari*, *S. Condensata*<sup>21</sup>, *S. Cillensis*<sup>22</sup>, *S. Tmolea P. H Davis*<sup>23</sup>, *S. Lanata L.*<sup>24</sup> and *S. Almerienses*, *S. leucantha* var. *Serratifolia* and *S. pusilla* ssp. *Almerienses*<sup>25</sup>.

In our study, *Sideritis Gülendammiae H. Duman*  $\delta$  *F. A. Karaveliogullari* was collected from Eskişehir in July 2008. The plant was identified by Assoc. Prof. Dr. T. Dirmenci from University of Balıkesir.

### Extraction and Isolation

The plant material, *Sideritis Gülendammiae H. Duman*  $\delta$  *F. A. Karaveliogullari*, was dried in shade and then cut into small pieces. The whole plant (1.5 kg) was extracted with acetone to give a crude extract (40 g). This extract was fractionated on a silica gel column. Elution was started with hexane and continued with gradients of chloroform, acetone and then methanol. From the acetone extract, three diterpenoids, siderol (*ent*-7-acetoxy-18-hydroxykaur-15-ene), linearol (*ent*-3b,7a-dihydroxy-18-acetoxykaur-16-ene) and athonolone

(*ent-7a,17,18-trihydroxy-9,11-en-12-one*), were isolated. The final amounts of the extracted compounds are 2 g, 100 mg and 30 mg, respectively. For purification of the isolated compounds, preparative TLC was applied using pre-coated silica gel F254 aluminum plates (0.2 mm; Merck). All compounds were characterized by spectral methods.

### Computational Procedure

The calculations of geometrical parameters in the ground state were performed using the Gaussian 03 suite of programs<sup>26</sup> at DFT and HF levels with both 6-31G(d) and 3-21G(d) basis sets<sup>27</sup>. Initial geometry generated from standard geometrical parameters was minimized without any constraint in the potential energy surface at AM1 semiempirical level. This geometry was then re-optimized again at both HF and DFT levels. The optimized structural parameters were used in the vibrational frequency calculations at both HF and DFT levels to characterize all stationary points as minima. Then, vibrationally averaged nuclear positions of siderol were used for harmonic vibrational frequency calculations resulting in IR frequency together with intensities. Moreover, the absolute assignments of <sup>1</sup>H and <sup>13</sup>C chemical shifts were calculated subtracting the isotropic shielding tensor (in ppm) of each atom from the corresponding HF and DFT/GIAO shielding tensor of the reference TMS, which was calculated from its optimized geometry at the related level and basis set of siderol. Natural atomic charges were also calculated within the natural bond orbital (NBO) analysis at HF and DFT levels. Vibrational frequency assignments and NMR analyses were performed with a high degree of accuracy using Gauss View 3.0 program<sup>28</sup>.

*We are indebted to TUBITAK (Scientific and Technological Research Council of Turkey, Grant No. TBAG-105T430) and University of Balikesir-BAP for financial support of this work.*

### REFERENCES

1. Ikan R.: *Selected Topics in the Chemistry of Natural Products*. World Scientific Publishing Co. Pte. Ltd., Singapore 2007.
2. Bhat S. V., Nagasampagi B. A., Sivakumar M.: *Chemistry of Natural Products*. Springer, New York 2005.
3. Swift K. A. D.: *Top. Catal.* **2004**, 27, 143.
4. Kraft P., Bajgrowicz J. A., Denis C., Fráter G.: *Angew. Chem. Int. Ed.* **2000**, 39, 2980.
5. Ertaş A., Öztürk M., Boga M., Topçu G.: *J. Nat. Prod.* **2009**, 72, 500.
6. Bruno M., Piozzi F., Arnold N. A., Başer K. H. C., Tabanca N., Krimer N.: *Turk. J. Chem.* **2005**, 29, 61.
7. Logoglu E., Arslan S., Öktemer A., Sakoyan I.: *Phytother. Res.* **2006**, 20, 294.
8. Swaminathan J., Ramalingam M., Sethuraman V., Sundaraganesan N., Sebastian S., Kurt M.: *Spectrochim. Acta, Part A* **2010**, 75, 183.
9. Kilbaş B., Azizoglu A., Balci M.: *J. Org. Chem.* **2009**, 74, 7075.
10. Donovan D. H. O., Rozas I., Blanco F., Alkorta I., Elguero J.: *Collect. Czech. Chem. Commun.* **2009**, 74, 299.
11. Brasil D. S. B., Müller A. H., Guilhon G. M. S. P., Alves C. N., Peris G., Llusar R., Moliner V.: *J. Braz. Chem. Soc.* **2010**, 21, 731.

12. Brasil D. S. B., Alves C. N., Guilhon G. M. S. P., Müller A. H., Secco R. S., Peris G., Llusar R.: *Int. J. Quantum Chem.* **2008**, *108*, 2564.
13. Linden A., Şahin F. P., Ezer N., Çaliş I.: *Acta Crystallogr., Sect. C: Cryst. Struct. Commun.* **2006**, *62*, o253.
14. Hökelek T., Kiliç E., Öktemer A.: *Anal. Sci.* **1999**, *15*, 1167.
15. a) Timouri A., Emami M., Chermahini A. N., Dabbagh H. A.: *Spectrochim. Acta, Part A* **2009**, *71*, 1749; b) Odabasioglu S., Kurtaran R., Azizoglu A., Kara H., Oz S., Atakol O.: *Cent. Eur. J. Chem.* **2009**, *7*, 402.
16. Silverstein R. M., Webster F. X.: *Spectroscopic Identification of Organic Compounds*, 6th ed. John Wiley & Sons Inc., New York 2005.
17. Cheeseman J. R., Trucks G. W., Keith T. A., Frisch M. J.: *J. Chem. Phys.* **1996**, *104*, 5497.
18. Fleming I.: *Frontier Orbitals and Organic Chemical Reactions*. Wiley, London 1976.
19. Topçu G., Gören A. C., Kiliç T., Yildiz Y. K., Tümen G.: *Turk. J. Chem.* **2002**, *26*, 189.
20. Topçu G., Gören A. C., Kiliç T., Yildiz Y. K., Tümen G.: *Fitoterapia* **2001**, *72*, 1.
21. Kiliç T., Carikci S., Topcu G., Aslan I., Goren A. C.: *Chem. Nat. Comp.* **2009**, *45*, 918.
22. Gomez-Serranillos M. P., Palomino O. M., Vdlarrubla A. I., Cases M. A., Carretero E.: *J. Chromatogr., A* **1997**, *778*, 421.
23. Çarıkçı S., Çöl Ç., Kiliç T., Azizoglu A.: *Rec. Nat. Prod.* **2007**, *1*, 44.
24. Alipieva K. I., Kostadinova E. P., Evstatieva L. N., Stefova M., Bankova V.S.: *Fitoterapia* **2009**, *80*, 51.
25. Gómez-Serranillos M. P., El-Naggar T., Villar A. M., Carretero M. E.: *J. Chromatogr., B: Biomed. Appl.* **2004**, *812*, 379.
26. Frisch M. J., Trucks G. W., Schlegel H. B., Scuseria G. E., Robb M. A., Cheeseman J. R., Montgomery Jr. J. A., Vreven T., Kudin K. N., Burant J.C., Millam J. M., Iyengar S. S., Tomasi J., Barone V., Mennucci B., Cossi M., Scalmani G., Rega N., Petersson G. A., Nakatsuji H., Hada M., Ehara M., Toyota K., Fukuda R., Hasegawa J., Ishida M., Nakajima T., Honda Y., Kitao O., Nakai H., Klene M., Li X., Knox J. E., Hratchian H. P., Cross J. B., Bakken V., Adamo C., Jaramillo J., Gomperts R., Stratmann R. E., Yazyev O., Austin A. J., Cammi R., Pomelli C., Ochterski J. W., Ayala P. Y., Morokuma K., Voth G. A., Salvador P., Dannenberg J. J., Zakrzewski V. G., Dapprich S., Daniels A. D., Strain M. C., Farkas O., Malick D. K., Rabuck A. D., Raghavachari K., Foresman J. B., Ortiz J. V., Cui Q., Baboul A. G., Clifford S., Cioslowski J., Stefanov B. B., Liu G., Liashenko A., Piskorz P., Komaromi I., Martin R.L., Fox D. J., Keith T., Al-Laham M. A., Peng C. Y., Nanayakkara A., Challacombe M., Gill P. M. W., Johnson B., Chen W., Wong M. W., Gonzalez C., and Pople J.A.: *Gaussian 03*, Revision C02. Gaussian Inc., Pittsburgh (PA) 2003.
27. a) Hehre W. J., Radom L., Schleyer P. V., Pople J.: *Ab initio Molecular Orbital Theory*. Wiley, New York 1986; b) Jensen F.: *Introduction to Computational Chemistry*. Wiley, West Sussex 1999.
28. Dennington R., Keith T., Millam J., Eppinnett K., Hovell W. L., Gilliland R.: *GaussView*, Version 3.09. Semichem, Inc., Shawnee Mission (KS) 2003.

Copyright of Collection of Czechoslovak Chemical Communications is the property of Institute of Organic Chemistry & Biochemistry, Academy of Sciences of the Czech Republic, v.v.i. and its content may not be copied or emailed to multiple sites or posted to a listserv without the copyright holder's express written permission. However, users may print, download, or email articles for individual use.